

Comparative Diagnostic Performance of ^{68}Ga -PSMA and ^{68}Ga -DOTA-RM2 PET/MRI in the Evaluation of Recurrent Prostate Cancer

Tien Yin Wong, Joseph J. Y. Sung, Joseph Lau, Paul K. S. Chan

Departments of Experimental Medicine and Infectious Diseases, Nanjing Drum Tower Hospital, Nanjing University Medical School, Nanjing 210008, China.

*E-mail ✉ Jos.jy.sung@163.com

Received: 02 February 2023; Revised: 19 April 2023; Accepted: 22 April 2023

ABSTRACT

This investigation compares how effectively ^{68}Ga -PSMA and ^{68}Ga -DOTA-RM2 PET/MRI identify prostate cancer (PCa) recurrence following initial therapy and examines how the results of these two tracers relate to clinical and pathological variables. Thirty-five men experiencing biochemical relapse (BCR) underwent restaging with ^{68}Ga -PSMA PET/MRI, and 31 of them also completed a ^{68}Ga -DOTA-RM2 PET/MRI examination within a period of up to 16 days (mean interval: 3 days; range: 2–16 days). Imaging obtained from both modalities was assessed qualitatively and quantitatively at the patient and lesion levels, and findings were verified through clinical evaluation and subsequent diagnostic follow-up. Statistical analyses were performed using Fisher's exact test and the Mann-Whitney U test, adopting a p-value threshold of <0.05 . The study population had an average age of 70 years (49–84) and a mean PSA concentration of 1.88 ng/mL at the time of imaging (0.21–14.4). Compared with ^{68}Ga -DOTA-RM2 PET/MRI, the ^{68}Ga -PSMA scan detected disease more frequently, revealing 95 lesions in 26 of 35 patients, while the RM2 tracer identified 41 lesions in 15 of 31 patients ($p = 0.016$ and 0.002). Among the 31 men who underwent both scans, 11 showed inconsistent results; 10 were positive only on ^{68}Ga -PSMA, and follow-up confirmed 9 of these as genuine recurrences, with 1 determined to be a false-positive finding. Higher PSA values and shorter PSA doubling time (DT) were associated with a greater number of ^{68}Ga -PSMA-avid lesions ($p = 0.006$ and 0.044), while no link emerged between imaging results and Gleason score. Overall, ^{68}Ga -PSMA PET/MRI demonstrated superior ability to identify recurrent PCa compared with ^{68}Ga -DOTA-RM2, and the burden of PSMA-positive lesions correlated with PSA metrics, suggesting a potential prognostic role.

Keywords: Prostate cancer; Recurrence; PSMA; RM2; PET/MRI

How to Cite This Article: Wong T Y, Eghbali T, Sung J J Y, Lau J, Chan P K S. Comparative Diagnostic Performance of ^{68}Ga -PSMA and ^{68}Ga -DOTA-RM2 PET/MRI in the Evaluation of Recurrent Prostate Cancer. Asian J Curr Res Clin Cancer. 2023;3(1):105-19. <https://doi.org/10.51847/Ibu5Dgs8Wp>

Introduction

Recurrence of prostate cancer (PCa) occurs in up to half of the men who initially undergo radical prostatectomy (RP) or external-beam radiotherapy (EBRT) for clinically localized disease [1]. Once biochemical recurrence (BCR) is identified, determining the precise site and burden of relapse becomes essential, as this guides clinicians toward targeted therapeutic options that can extend cancer-free survival and potentially defer systemic treatments such as androgen deprivation therapy [2].

Serum Prostate Specific Antigen (PSA) is the standard biomarker used to detect BCR, yet it does not reveal where recurrent disease is located. Importantly, men with low PSA levels may benefit most from early localized salvage approaches, although conventional imaging techniques show poor sensitivity for detecting recurrence when PSA is below 1 ng/mL [1]. In contrast, individuals with metastatic spread require systemic management, making the

ability to distinguish localized from disseminated disease crucial for treatment planning [3]. Consequently, imaging plays a central role in characterizing both local and distant lesions.

During the past decade, Prostate Specific Membrane Antigen (PSMA)—a transmembrane molecule markedly upregulated in PCa cells—has become a leading PET imaging target. Radiotracers directed at PSMA offer superior sensitivity and specificity for identifying metastatic sites, even at low PSA concentrations, outperforming conventional imaging modalities [4-6].

In addition to PSMA, gastrin-releasing peptide receptors (GRPR), which are G-protein coupled receptors expressed at elevated levels in prostate tumors at both mRNA and protein levels, have emerged as alternative molecular imaging targets [7]. Among various GRPR-binding compounds, ^{68}Ga -DOTA-RM2 is the most extensively evaluated tracer to date [8-11].

Only a limited number of studies have explored combined PSMA- and GRPR-targeted imaging in PCa, either during initial staging [11, 12] or at the time of recurrence [9, 13]. Most of these investigations relied on PET/computed tomography (CT) systems for image acquisition [9, 12, 13].

The development of fully integrated PET/Magnetic Resonance Imaging (MRI) systems has introduced a new diagnostic approach for evaluating recurrent PCa. By acquiring PET and multiparametric MRI (mp-MR) simultaneously, PET/MRI offers metabolic, anatomical, and functional information in a single whole-body session while providing improved soft-tissue contrast and decreased radiation exposure compared with PET/CT [14, 15]. Nevertheless, evidence regarding its performance in this clinical context remains sparse, and studies employing both ^{68}Ga -PSMA and ^{68}Ga -DOTA-RM2 using PET/MRI remain particularly uncommon [9, 11, 13]. Given these gaps, the present study aimed to directly compare ^{68}Ga -PSMA and ^{68}Ga -DOTA-RM2 PET/MRI for detecting PCa recurrence after primary therapy. A secondary objective was to analyze how positive findings on either tracer correlate with clinical variables and histopathological features.

Materials and Methods

Patients

This prospective investigation enrolled 35 consecutive men with biochemical recurrence of PCa between June 2020 and March 2021 at the IRCCS San Raffaele Scientific Institute. Eligibility criteria included age above 18 years, previous definitive therapy for PCa, and biochemical failure defined as two PSA measurements ≥ 0.2 ng/mL following RP or an increase of ≥ 2 ng/mL above the PSA nadir for patients previously treated with radiotherapy (RT) [16].

Patients were excluded if they had medical conditions that could interfere with participation or if they had contraindications to MRI, such as severe claustrophobia.

All participants underwent ^{68}Ga -PSMA PET/MRI, and 31 of the 35 also completed a ^{68}Ga -DOTA-RM2 PET/MRI examination, with a minimum interval of 48 hours between sessions. PSA levels at several time points and Gleason Score (GS) after RP, when available, were documented for each patient.

Ethical approval for the study was obtained from the Institutional Ethics Committee of the IRCCS San Raffaele Scientific Institute (EudraCT 2018-001036-21). Written informed consent was collected from all participants. The data reported here represent part of a larger ongoing single-centre study conducted at IRCCS San Raffaele Scientific Institute (Project GR-2016-02363991).

^{68}Ga -PSMA PET/MRI acquisition protocol

^{68}Ga -PSMA was produced following the previously published synthesis method [11].

Patients were asked to fast on the day of their ^{68}Ga -PSMA PET/MRI examination. All scans were performed on a fully integrated 3-Tesla PET/MRI system (SIGNA PET/MRI; General Electric Healthcare, Waukesha, WI, USA) covering the region from the skull base to the mid-thigh.

Image acquisition began roughly one hour after tracer administration (mean \pm SD: 63 ± 17 min), following an injected activity between 129 and 288 MBq (mean \pm SD: 170.56 ± 36.06 MBq) of ^{68}Ga -PSMA [9, 13].

The protocol included a 20-minute high-statistics pelvic acquisition, restricted to a single bed position and paired with multiple MRI sequences obtained simultaneously:

- axial T2-weighted, large FOV: FSE; TR 10,235 ms; TE 99.7 ms; FOV 32×32 cm²; voxel $0.9 \times 0.9 \times 5$ mm³
- axial T2-weighted, small FOV: PROPELLER; TR 9578 ms; TE 151 ms; FOV 18×18 cm²; voxel $0.6 \times 0.6 \times 3$ mm³

- sagittal T2-weighted, small FOV: PROPELLER; TR 9578 ms; TE 151 ms; FOV $18 \times 18 \text{ cm}^2$; voxel $0.6 \times 0.6 \times 3 \text{ mm}^3$
- small-FOV DWI: TR 6643 ms; TE 79.5 ms; FOV $18 \times 18 \text{ cm}^2$; voxel $1.8 \times 1.8 \times 3 \text{ mm}^3$; b-values 50, 800, 1400, 2000 s/mm²; with ADC maps
- whole-pelvis T1 Lava Flex (pre- and post-contrast): TR 5 ms; TE 1.7 ms; FOV $44 \times 35.2 \text{ cm}^2$; voxel $1.3 \times 1.2 \times 2 \text{ mm}^3$
- dynamic contrast-enhanced T1 perfusion (after 0.1 mmol/kg gadobutrol bolus at 3.5 mL/s): DISCO; TR 5.1 ms; TE 1.7 ms; FOV $29 \times 29 \text{ cm}^2$; voxel $1.9 \times 2.2 \times 3 \text{ mm}^3$; 88 dynamics

After the pelvic HS sequence, a whole-body PET scan (5–6 bed positions, 4 min/position) was conducted in combination with whole-body MR imaging (T1 Lava Flex and DWI with $b = 50$ and 1000 s/mm^2).

PET reconstruction used a Bayesian penalized-likelihood method that incorporated both PSF and TOF modeling; reconstructions were generated with a 60-cm FOV and a 192×192 matrix.

Attenuation correction relied on the MR-based AC procedure applied to the simultaneously obtained LAVA-Flex images.

^{68}Ga -DOTA-RM2 PET/MRI acquisition protocol

^{68}Ga -DOTA-RM2 was synthesized according to previously published methodology [11].

This scan was performed within a maximum of sixteen days after the ^{68}Ga -PSMA PET/MRI examination (mean interval: 3 days; range: 2–16 days). Patients again followed fasting requirements, and the same PET/MRI system was used.

Imaging began about 50 minutes after tracer injection (mean \pm SD: 49 ± 13 min), following administration of $84\text{--}228 \text{ MBq}$ (mean \pm SD: $153.36 \pm 36 \text{ MBq}$) of ^{68}Ga -DOTA-RM2 [9, 13].

The protocol included a 20-minute high-statistics pelvic acquisition (single bed position), together with an axial large-FOV T2-weighted sequence ($32 \times 32 \text{ cm}^2$) for anatomical detail.

A whole-body PET scan (5–6 FOVs, 4 min/FOV) was then performed from the skull base to mid-thigh, acquired simultaneously with whole-body Lava Flex MRI and DWI sequences using b-values of 50 and 1500 s/mm^2 .

PET image reconstruction and attenuation correction followed exactly the same algorithms and technical parameters used for ^{68}Ga -PSMA PET.

PET/MR image analysis

Interpretation of ^{68}Ga -PSMA and ^{68}Ga -DOTA-RM2 PET/MR datasets was carried out on the Advantage Workstation (General Electric Healthcare). All PET, MRI, and fused PET/MR images were reviewed in axial, sagittal, and coronal orientations.

Two Nuclear Medicine specialists, each with more than 10 years of experience, performed the qualitative evaluation of both the pelvic HS acquisition and the whole-body scans, with full access to patient clinical information. MRI examinations—performed as part of clinical assessment—were interpreted separately by a radiologist, and each patient received a standard MRI report. Since the purpose of this study focused exclusively on PET tracers in recurrent prostate cancer, MRI findings were excluded from the analytical dataset and used solely for lesion localization.

Whole-body biodistribution of both tracers was assessed, noting any abnormal uptake suggestive of malignancy, except in regions known for physiologic tracer accumulation [17, 18]. Anatomical identification of lesions was performed using the simultaneously acquired MR images.

ROIs were semi-automatically placed on transaxial PET views: for patients with a single lesion, the ROI encompassed that site; for those with multiple abnormalities, the ROI was positioned over the lesion showing the most representative uptake pattern. From each ROI, SUVmax and SUVmean (using a 40% SUVmax threshold [19]) were extracted for both tracers from the whole-body PET acquisitions.

Comparative evaluation of tracer performance was conducted by examining whether both tracers detected the same abnormal sites. Findings were labeled as:

- concordant — identical lesions detected or both scans negative
- partially concordant — at least one, but not all, lesions identified by both tracers
- discordant — uptake visible with only one tracer but not the other

Lesion Validation

Verification of PET abnormalities was carried out through a combination of clinical assessment and imaging-based follow-up. A lesion detected on ⁶⁸Ga-PSMA or ⁶⁸Ga-DOTA-RM2 PET/MRI was classified as *true positive* when at least one of the following conditions applied:

- histopathology demonstrated malignancy in a surgically excised specimen;
- subsequent ⁶⁸Ga-PSMA PET/CT or PET/MRI showed progression—either an increase in the number of abnormal foci or a rise in uptake intensity—together with a concurrent PSA elevation;
- confirmation was obtained on other imaging modalities, either at baseline (including the diagnostic pelvic MRI acquired simultaneously with the ⁶⁸Ga-PSMA scan) or during serial follow-up;
- marked reduction or disappearance of abnormal ⁶⁸Ga-PSMA uptake was seen on later PET/CT or PET/MRI following local or systemic therapy, accompanied by a PSA decline of more than 50%;
- PSA decreased by more than 50% after targeted irradiation of the region showing pathological uptake on either radiotracer.

Patients showing no abnormal uptake on ⁶⁸Ga-PSMA and/or ⁶⁸Ga-DOTA-RM2 PET/MRI were considered *true negative* provided that conventional imaging and follow-up ⁶⁸Ga-PSMA PET/CT or PET/MRI continued to demonstrate no evidence of recurrent disease. For both positive and negative PET findings, the average duration of follow-up was 13.8 months (range 8.2–17.9 months).

Statistical analyses

All statistical procedures were carried out using R software [20] and Python 3.7 (Python Software Foundation, available at <http://www.python.org>, accessed 30 November 2021).

To assess differences in patient-level detection rates between ⁶⁸Ga-PSMA and ⁶⁸Ga-DOTA-RM2 PET/MRI among subjects who received both tracers, McNemar's test was applied. In the same subgroup, the Wilcoxon signed-rank test was used to compare the number of lesions detected by each radiotracer.

For evaluating associations between clinical characteristics and PET findings, patients were stratified according to:

- PSA level: ≤ 0.5 ng/mL, 0.5–2 ng/mL, and ≥ 2 ng/mL;
- PSA doubling time (PSA-DT): < 6 months vs. ≥ 6 months;
- Gleason score (GS) prior to radical treatment: GS $\leq 3+4$ vs. GS $\geq 4+3$.

Fisher's exact test was employed to examine relationships between clinical/histopathological variables and dual-tracer PET positivity at the patient level. Receiver Operating Characteristic (ROC) curves were also generated to determine the predictive value of PSA, PSA-DT, and GS for ⁶⁸Ga-PSMA and ⁶⁸Ga-DOTA-RM2 PET/MRI positivity, with area under the curve (AUC) and 95% confidence intervals calculated.

The Mann–Whitney U test was used to assess whether higher PSA, higher GS, or shorter PSA-DT correlated with a greater number of PET-positive lesions. All p-values were corrected for multiple comparisons using the false discovery rate method, and a threshold of $p < 0.05$ was considered statistically significant.

Results and Discussion

Patients

A total of thirty-five men with biochemical recurrence of prostate cancer were prospectively included. Their average age was 70 years (range 49–84). At the time of PET/MRI imaging, the mean PSA concentration was 1.88 ng/mL (range 0.21–14.4).

All patients underwent ⁶⁸Ga-PSMA PET/MRI, whereas 31 out of the 35 also completed the ⁶⁸Ga-DOTA-RM2 PET/MRI examination, with four individuals not undergoing the second scan because of limited compliance with the study protocol.

Table 1. Patients' characteristics.

Pt	Age (years)	GS	PSA (ng/mL)	Treatment	Adjuvant Therapy
1	64	4 + 4	9.86	RP	None
2	66	4 + 3	0.53	RP	None
3	75	3 + 3	0.54	RP	None

4	78	4 + 5	0.212	RP	RT
5	73	4 + 3	4.75	RP	RT
6	77	4 + 4	0.237	RP	None
7	58	4 + 3	1.3	RP	None
8	64	4 + 3	2.5	RP	RT
9	79	4 + 5	2	RP	RT; ADT
10	49	4 + 5	0.82	RP	None
11	84	NA	3.24	RT	None
12	79	5 + 3	1.53	RP	RT; ADT
13	75	3 + 4	0.39	RP	None
14	78	4 + 5	0.5	RP	RT
15	76	4 + 5	0.41	RP	RT
16	67	4 + 4	2	RP	None
17	76	3 + 4	0.41	RP	None
18	81	NA	3.53	RT	None
19	71	4 + 3	4.3	RP	RT
20	72	3 + 4	0.22	RP	RT
21	77	2 + 4	1.21	RP	None
22	77	4 + 5	4.63	RP	RT
23	50	5 + 5	14.4	RP	None
24	69	4 + 5	0.2	RP	None
25	59	4 + 4	0.26	RP	None
26	53	NA	0.25	RP	None
27	75	4 + 3	0.27	RP	None
28	62	3 + 3	0.68	RP	None
29	70	5 + 4	2.16	RP	None
30	73	4 + 3	0.4	RP	None
31	64	4 + 5	0.23	RP	None
32	69	NA	0.37	RP	RT
33	74	5 + 4	0.74	RP	RT
34	62	5 + 4	0.34	RP	RT
35	60	4 + 3	0.48	RP	None

RP: radical prostatectomy; RT: radiotherapy; LN: lymph-node; ADT: androgen deprivation therapy; PSA at time of scans; NA: not available.

PET/MRI findings and comparison between ⁶⁸Ga-PSMA and ⁶⁸Ga-DOTA-RM2

In the cohort, ⁶⁸Ga-PSMA PET/MRI detected recurrent prostate cancer in 26 out of 35 patients, corresponding to a detection rate of 74%, with a total of 95 lesions identified. The lesions showed a mean SUVmax of 19.69 (range 1.91–112.37) and a mean SUVmean of 12.03 (range 1.04–65.83). By comparison, ⁶⁸Ga-DOTA-RM2 PET/MRI was positive in 15 of the 31 patients who underwent this scan, resulting in 41 lesions in total, with a mean SUVmax of 19.51 (range 3.41–146.62) and a mean SUVmean of 13.36 (range 2.04–101.41). When comparing findings between the two tracers in the 31 patients who received both scans, results were fully concordant in 12 cases, with six patients showing identical positive findings on both examinations and six patients having negative scans on both modalities. Eight patients exhibited partial concordance, where only some lesions were detected by both tracers, while 11 patients showed discordant results. In these discordant cases, ⁶⁸Ga-PSMA PET/MRI identified seven lesions in five patients with local recurrence, five lesions in five patients with bone metastases, four lesions in three patients with lymph node involvement, and two lesions in one patient with visceral metastasis. In contrast, ⁶⁸Ga-DOTA-RM2 PET/MRI detected a single lesion in one patient with bone disease. **Figure 1** provides an example of PET/MRI imaging for reference.

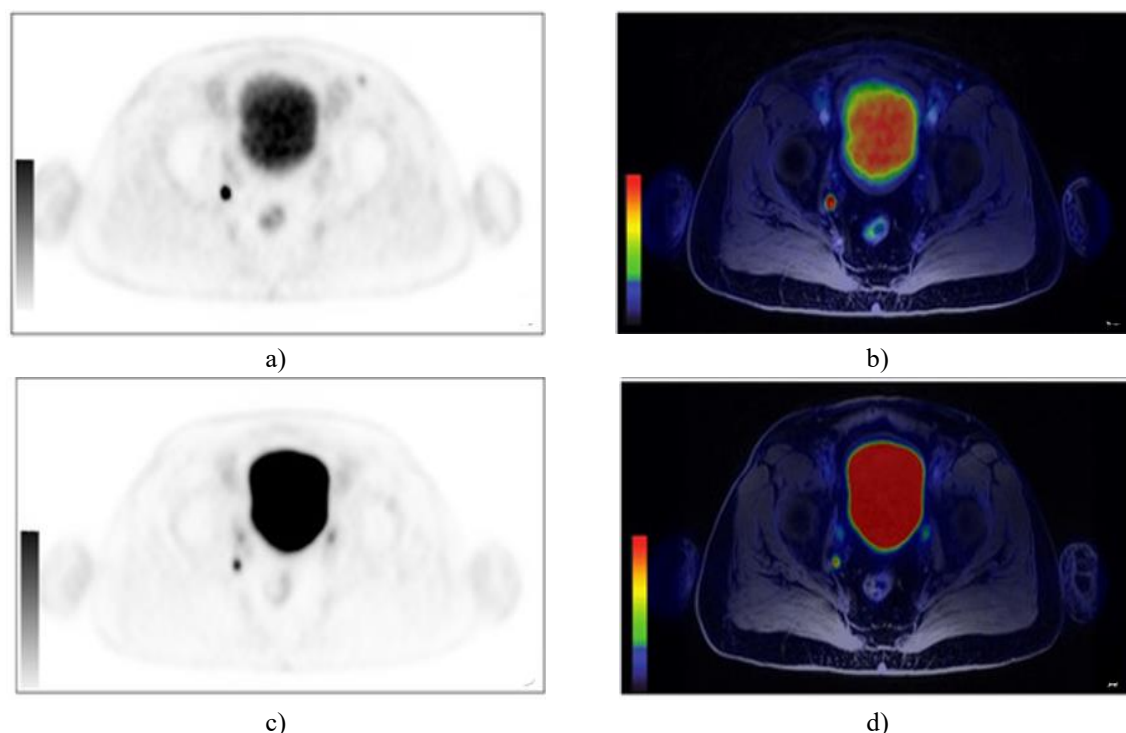


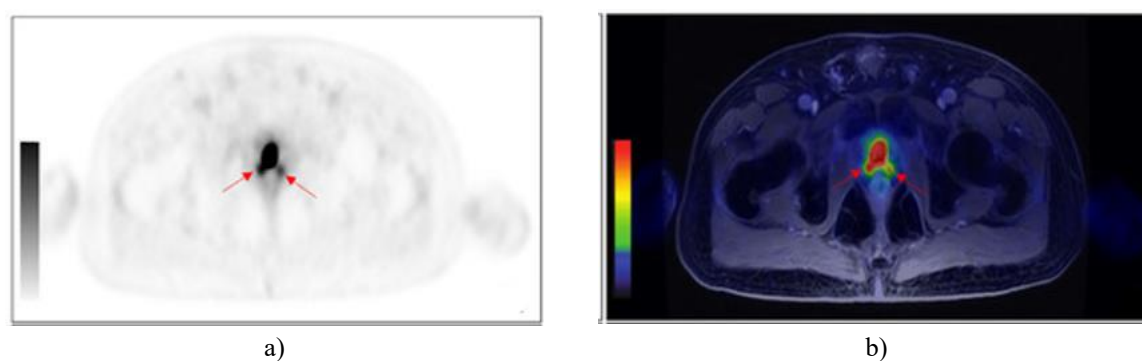
Figure 1. Example of Concordant PET/MRI Findings in Lymph Node Recurrence

Figure 1 illustrates a case of concordant detection of lymph nodal recurrence using both ^{68}Ga -PSMA and ^{68}Ga -DOTA-RM2 PET/MRI. The patient, a 66-year-old man previously treated with radical prostatectomy for a Gleason 7 (4+3) prostate cancer (pT3aN0), experienced biochemical recurrence with a PSA level of 0.53 ng/mL. The ^{68}Ga -PSMA PET/MRI demonstrated a focal uptake in the right obturator lymph node, visible on axial PET images (a) and axial fused PET/MRI images (b). The same pathological focus was detected on the ^{68}Ga -DOTA-RM2 PET/MRI scans, as shown in the axial PET (c) and axial PET/MRI (d) images.

Among the twelve patients with fully concordant findings, six were confirmed as true positive and four as true negative, while two were ultimately classified as false negative. Of particular interest, in patient number nine, who was confirmed true positive, follow-up conventional imaging revealed only a subset of the lesions that had been identified by PET with both radiotracers.

In the subset of patients showing partial concordance between the tracers, only one individual demonstrated additional lesions on ^{68}Ga -DOTA-RM2 compared to ^{68}Ga -PSMA; however, these extra findings were not corroborated by evidence obtained during follow-up. Conversely, in five of the seven patients in whom ^{68}Ga -PSMA identified more sites of recurrence than ^{68}Ga -DOTA-RM2, the additional lesions were confirmed by subsequent follow-up examinations.

Among the eleven cases showing discordant findings, ten were positive on ^{68}Ga -PSMA while negative on ^{68}Ga -DOTA-RM2, with representative images provided in **Figures 2 and 3**.



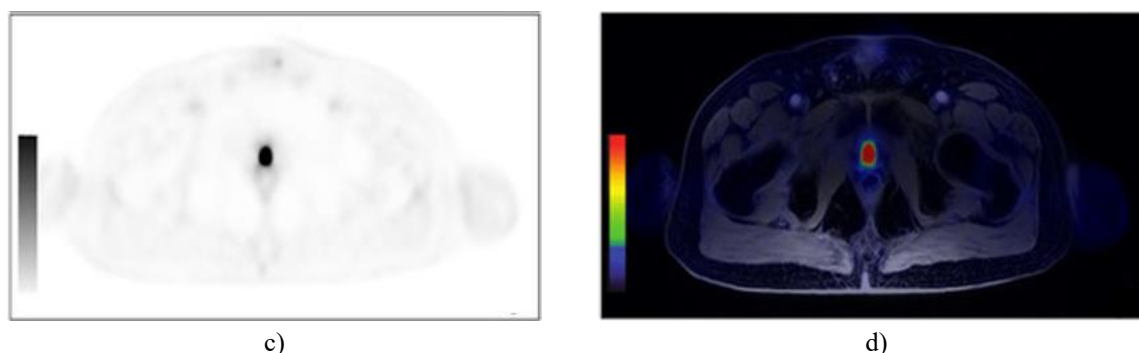


Figure 2. Example of Discordant PET/MRI Findings in Local Recurrence

Figure 2 depicts a case of discordant detection between ^{68}Ga -PSMA and ^{68}Ga -DOTA-RM2 PET/MRI in a patient with local prostate cancer recurrence. The patient, a 64-year-old man previously treated with radical prostatectomy for Gleason 4+3 prostate cancer, presented with biochemical recurrence, with a PSA level of 2.5 ng/mL. The ^{68}Ga -PSMA PET/MRI demonstrated pathological radiotracer uptake in the posterior regions of the prostatic bed on both the right and left sides, as indicated by red arrows on the axial PET (a) and fused axial PET/MRI (b) images. In contrast, the ^{68}Ga -DOTA-RM2 PET/MRI images showed no abnormal uptake in the same region, as illustrated on the axial PET (c) and fused axial PET/MRI (d) images.

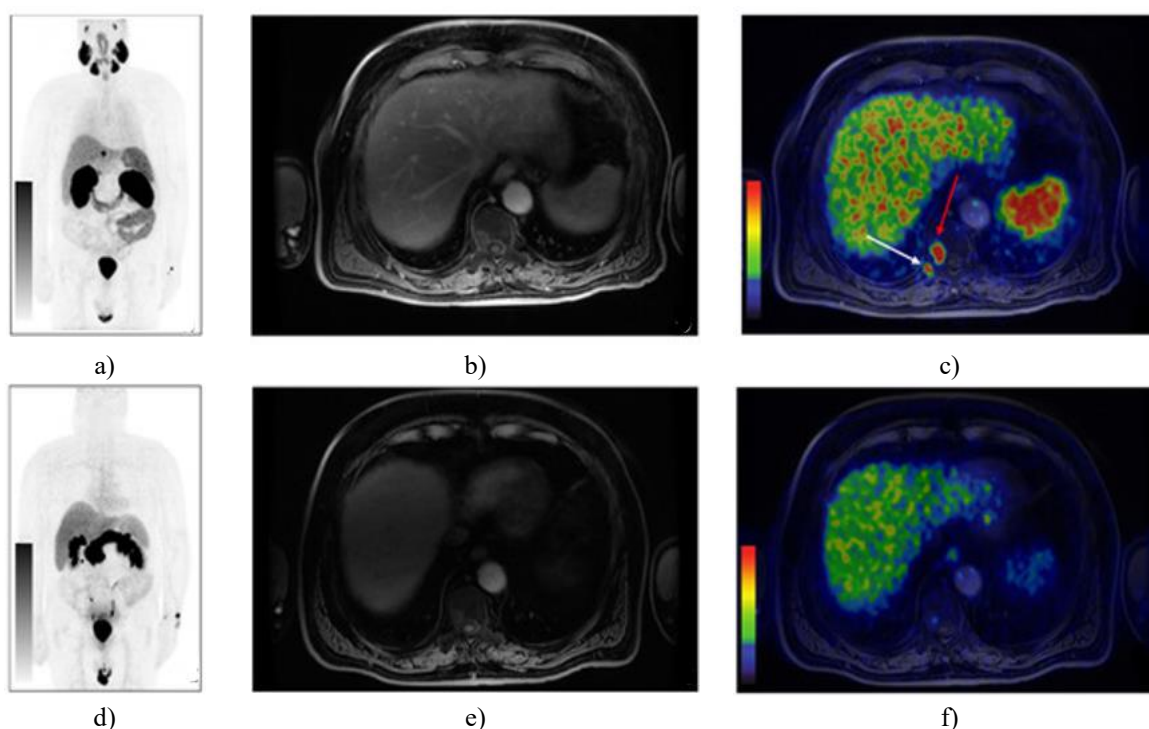


Figure 3. Example of Discordant PET/MRI Findings in Bone Metastases Detection

Figure 3 illustrates a case of discordant findings between ^{68}Ga -PSMA and ^{68}Ga -DOTA-RM2 PET/MRI in the evaluation of bone metastases. The patient, a 70-year-old man previously treated with radical prostatectomy for Gleason 5+4 prostate cancer (pT3aN0), experienced biochemical recurrence with a PSA of 2.16 ng/mL. The ^{68}Ga -PSMA PET/MRI demonstrated abnormal radiotracer uptake at the right D10 vertebral hemisome, visible on the maximum intensity projection (MIP) image (a), the axial LAVA-FLEX MRI (b), and the fused axial PET/MRI (c, red arrow). Additional uptake was noted in the right posterior segment of the tenth rib (c, white arrow). In contrast, the ^{68}Ga -DOTA-RM2 PET/MRI images showed no significant tracer accumulation, as seen on the MIP (d), axial LAVA-FLEX MRI (e), and fused PET/MRI (f) images.

Among the eleven patients presenting discordant findings in bone lesions, nine of the ten ^{68}Ga -PSMA positive cases were confirmed as true positive based on follow-up examinations, while one lesion identified by ^{68}Ga -PSMA

was not supported by subsequent evidence and was therefore classified as false positive. The single patient with a ^{68}Ga -DOTA-RM2 positive lesion but negative ^{68}Ga -PSMA scan was ultimately verified as a true positive. Detailed follow-up data for each patient are provided in **Table 2**.

Table 2. PET findings and PET findings validation.

Patient (Pt)	^{68}Ga -PSMA PET Findings	^{68}Ga -DOTA-RM2 PET Findings	Validation of PET Findings**
1	Left perirectal lesion	Left perirectal lesion	Confirmed by baseline conventional imaging
2	Right obturator LN; right laterocervical LN	Right obturator LN	Right obturator LN confirmed by baseline conventional imaging
3	Negative	Negative	No disease on baseline or follow-up conventional imaging
4	Left humerus	Not assessed	>50 % PSA decline after radiotherapy at the site of pathological ^{68}Ga -PSMA uptake
5	Left supraclavicular LN; 2 left para-aortic LNs; left iliac bone; left sacral ala	Left synchondrosis; 8 left para-aortic LNs; inter-aortocaval LN; left retroclavicular LN; 2 right retrocrural LNs; 2 left common iliac LNs	Left iliac bone and left sacral ala confirmed by baseline conventional imaging
6	Negative	Not assessed	No disease on baseline or follow-up conventional imaging; stable PSA during follow-up
7	Negative	Negative	No disease on baseline or follow-up conventional imaging, ^{11}C -choline PET, or ^{68}Ga -PSMA PET
8	Bilateral prostatic fossa (2 sites)	Negative	Progression on follow-up ^{68}Ga -PSMA PET with rising PSA
9	Left lateral rectal wall; left common iliac LN; left paramedian presacral LN	Left lateral rectal wall; left common iliac LN; left paramedian presacral LN	Left lateral rectal wall confirmed by baseline conventional imaging
10	Right iliac ala	Not assessed	>50 % PSA decline after radiotherapy at the site of pathological ^{68}Ga -PSMA uptake
11	Right prostate lobe; right internal iliac LN; left iliac bone	Right prostate lobe	Disappearance of ^{68}Ga -PSMA uptake on follow-up PET after systemic therapy with >50 % PSA decline
12	Right vesico-urethral anastomosis; 2 left laterocervical LNs; left retroclavicular LN; left dorsal LN	Right vesico-urethral anastomosis	Right vesico-urethral anastomosis confirmed by baseline conventional imaging
13	Right vesico-urethral anastomosis; left common iliac LN	Left common iliac LN	^{68}Ga -PSMA findings confirmed by baseline conventional imaging
14	Negative	Negative	Disease evident on baseline conventional imaging (vesico-urethral anastomosis & right iliac bone) with rising PSA during follow-up
15	Right vesico-urethral anastomosis	Negative	^{68}Ga -PSMA findings confirmed by baseline conventional imaging
16	Left pubis; right V rib	Negative	Left pubis confirmed by baseline conventional imaging
17	Negative	Not assessed	Disease present on baseline conventional imaging (vesico-urethral anastomosis)

18	Negative	Negative	No disease on baseline or follow-up conventional imaging
19	Left pulmonary hilum; left acetabulum	Left pulmonary hilum	Disappearance of ⁶⁸ Ga-PSMA uptake on follow-up PET after systemic therapy with >50 % PSA decline
20	Left retrolateral vesico-urethral anastomosis	Negative	⁶⁸ Ga-PSMA findings confirmed by baseline conventional imaging
21	Left obturator LN; left III rib	Left obturator LN; left III rib	Both sites confirmed by baseline conventional imaging
22	Bilateral iliac LNs (2); left rectus abdominis muscle; bilateral pleura (2)	Negative	⁶⁸ Ga-PSMA findings confirmed by baseline conventional imaging; pleural lesions confirmed histologically in resected specimens
23	Multiple LNs (16); multiple skeletal lesions (27)	Left retroclavicular LN; left para-aortic LN; multiple hips (6)	Multiple LN and skeletal lesions confirmed by baseline conventional imaging
24	Right perirectal LN; right pubic bone	Negative	⁶⁸ Ga-PSMA findings confirmed by baseline conventional imaging
25	Small trochanter	Negative	⁶⁸ Ga-PSMA findings confirmed by baseline conventional imaging and >50 % PSA decline after radiotherapy at the site
26	Negative	Negative	Disease present on baseline conventional imaging (para-aortic & aortocaval LN)
27	Right VIII rib	Negative	No disease on baseline or follow-up conventional imaging
28	D7 right hemisome	Negative	⁶⁸ Ga-PSMA findings confirmed by baseline conventional imaging
29	D10 right hemisome; right X rib; D8	D10 right hemisome	⁶⁸ Ga-PSMA findings confirmed by baseline conventional imaging
30	Negative	Negative	No disease on baseline or follow-up conventional imaging
31	Negative	Right thigh bone	⁶⁸ Ga-DOTA-RM2 findings confirmed by baseline conventional imaging
32	Paracaval LN	Negative	⁶⁸ Ga-PSMA findings confirmed by baseline conventional imaging
33	Right iliac LN; 2 right obturator LNs	Right iliac LN; 2 right obturator LNs	All sites confirmed by baseline conventional imaging; disappearance of ⁶⁸ Ga-PSMA uptake on follow-up PET after systemic therapy with >50 % PSA decline
34	Left IX rib	Left IX rib	Confirmed by baseline conventional imaging
35	Right obturator LN	Right obturator LN	Confirmed by baseline conventional imaging

LN: lymph node; NA: not available.

Across the 31 patients who underwent both scans, a total of 26 lesions were detected by both ⁶⁸Ga-PSMA and ⁶⁸Ga-DOTA-RM2 PET/MRI in 19 patients. In addition, ⁶⁸Ga-PSMA identified 66 further lesions in 17 patients that were not visualized with ⁶⁸Ga-DOTA-RM2, whereas 15 lesions in three patients were observed exclusively on ⁶⁸Ga-DOTA-RM2 PET/MRI. Analysis of patient-based detection rates, illustrated in **Figure 4a**, and the mean number of lesions detected per patient, shown in **Figure 5a**, revealed statistically significant differences between the two imaging modalities ($p = 0.016$ and 0.002 , respectively). Detection rates stratified by serum PSA level, PSA doubling time, and Gleason score prior to radical therapy are presented in **Figures 4b and 4c**, and **4d**, respectively. Furthermore, **Figure 5b** displays the average number of lesions detected by the two tracers according to the anatomical site of recurrence.

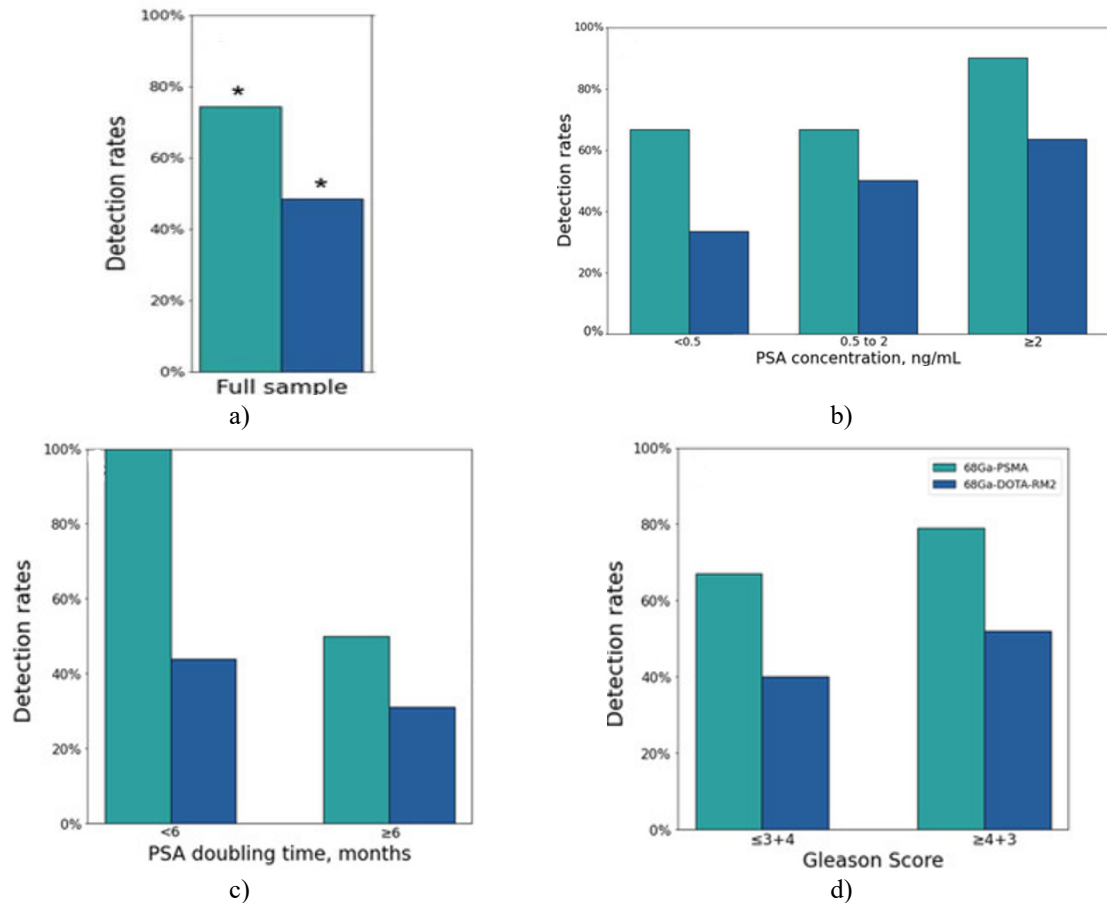


Figure 4. illustrates the comparative findings of ^{68}Ga -PSMA and ^{68}Ga -DOTA-RM2 PET/MRI. Panel (a) shows the overall patient-based detection rates for the two radiotracers. Panels (b), (c), and (d) display detection rates stratified according to serum PSA levels at the time of imaging, PSA doubling time, and Gleason score prior to radical treatment, respectively. Statistically significant differences between the tracers are indicated by an asterisk (*), representing $p < 0.05$.

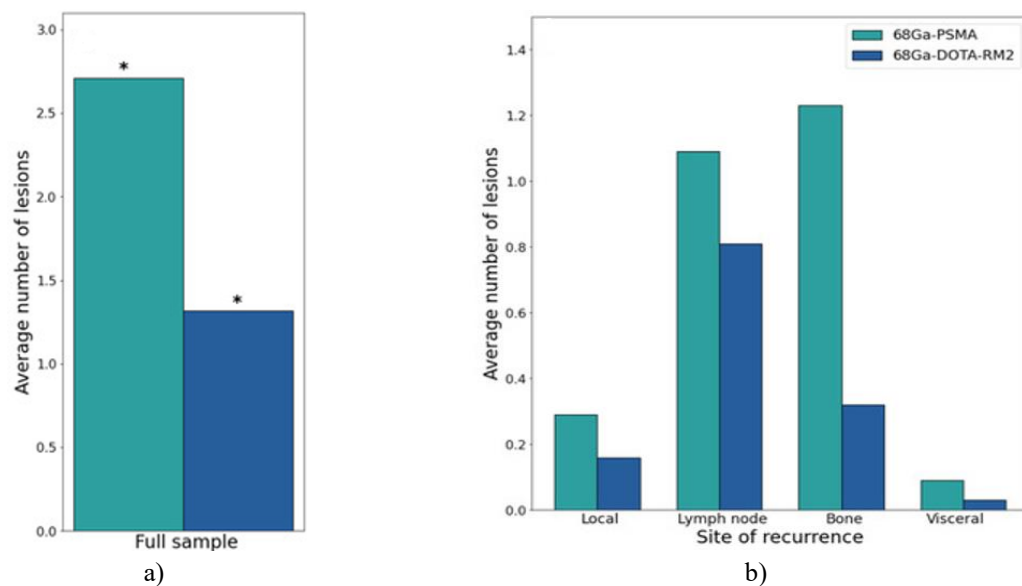


Figure 5. Lesion-Level Findings of ^{68}Ga -PSMA and ^{68}Ga -DOTA-RM2 PET/MRI

Figure 5 presents the comparison of ^{68}Ga -PSMA and ^{68}Ga -DOTA-RM2 PET/MRI at the lesion level. Panel (a) shows the mean number of lesions detected by each radiotracer, while panel (b) illustrates the average number of positive lesions stratified according to the anatomical site of recurrence. Statistically significant differences are indicated by an asterisk (*), corresponding to $p < 0.05$.

Associations between semi-quantitative PET parameters and clinical variables

The relationships between patient clinical characteristics and detection rates of ^{68}Ga -PSMA and ^{68}Ga -DOTA-RM2 PET/MRI are summarized in **Table 3**. There was no significant association between PSA levels or Gleason score and ^{68}Ga -PSMA PET/MRI positivity. However, patients with longer PSA doubling times were less likely to exhibit positive ^{68}Ga -PSMA PET findings compared to those with PSA DT shorter than six months ($\text{OR} < 0.01$, $p = 0.022$). This association, however, did not remain statistically significant after adjustment for multiple comparisons (adjusted $p = 0.065$). None of the clinical variables analyzed demonstrated a significant correlation with ^{68}Ga -DOTA-RM2 PET/MRI positivity at the patient level.

Table 3. Correlations between ^{68}Ga -PSMA and ^{68}Ga -DOTA-RM2 detection rates and clinical data on a patient basis.

Imaging Modality	Stratification	No. of Patients	Positive Results, No. (%)	p Value	Adjusted p Value
^{68}Ga -PSMA PET/MRI	PSA			0.339	0.509
	<0.5	15	10 (67)		
	0.5–2	9	6 (67)		
	≥ 2	11	10 (91)		
	PSA DT			0.022	0.065
	<6	9	9 (100)		
	≥ 6	16	8 (50)		
	Not available	10	9 (90)		
	GS			0.603	0.603
	$\leq 3 + 4$	6	4 (67)		
	$\geq 4 + 3$	24	19 (79)		
	Not available	5	3 (60)		
^{68}Ga -DOTA-RM2 PET/MRI	PSA			0.390	0.993
	<0.5	12	4 (33)		
	0.5–2	8	4 (50)		
	≥ 2	11	7 (64)		
	PSA DT			0.662	0.993
	<6	9	4 (44)		
	≥ 6	13	4 (31)		
	Not available	9	7 (78)		
	GS			1	1
	$\leq 3 + 4$	5	2 (40)		
	$\geq 4 + 3$	21	11 (52)		
	Not available	5	2 (40)		

PSA: Prostate Specific Antigen (ng/mL); PSA DT: PSA Doubling Time (months); GS: Gleason Score.

Figure 6 illustrates the area under the curve (AUC) and corresponding 95% confidence intervals for each clinical variable in predicting positive ^{68}Ga -PSMA (**Figure 6a**) or ^{68}Ga -DOTA-RM2 (**Figure 6b**) PET/MRI results in recurrent prostate cancer. PSA doubling time demonstrated an AUC of 0.77 (95% CI: 0.58–0.96) for predicting ^{68}Ga -PSMA PET positivity. For ^{68}Ga -DOTA-RM2 PET, PSA levels at the time of imaging showed an AUC of 0.69; however, the 95% confidence interval approached the diagonal line, indicating performance near random classification. None of the other clinical parameters evaluated exhibited significant predictive value for positivity of either ^{68}Ga -PSMA or ^{68}Ga -DOTA-RM2 PET/MRI in detecting recurrent prostate cancer in this cohort.

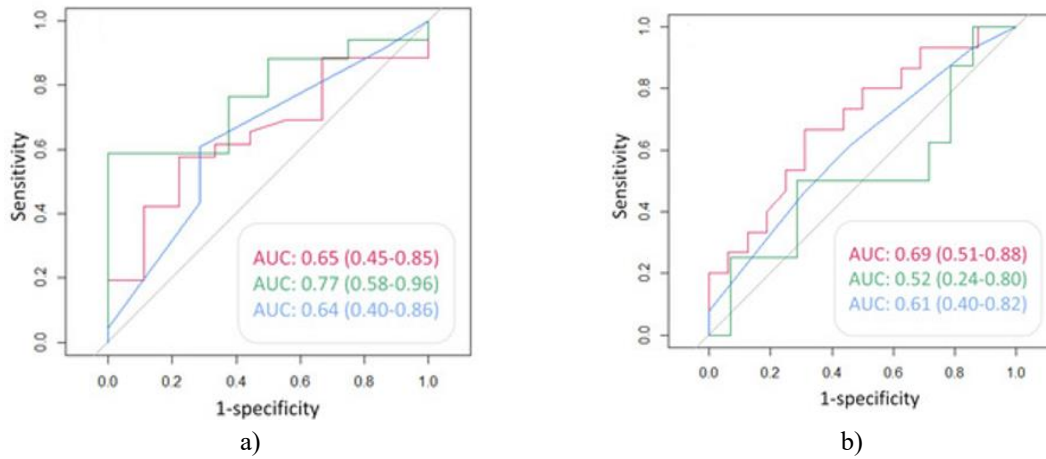


Figure 6. ROC analysis for the prediction of (a): ^{68}Ga -PSMA and (b): ^{68}Ga -DOTA-RM2 PET positive findings. Red line: AUC of PSA at time of scans in the prediction of PET positivity; green line: AUC of PSA DT in the prediction of PET positivity; blue line: AUC of GS prior to radical treatment in the prediction of PET positivity. AUC and 95% CI are here reported.

Table 4 reports the number of lesions detected by PET/MRI stratified according to GS, PSA levels and kinetic.

Table 4. Study of the differences in the number of lesions detected by ^{68}Ga -PSMA and ^{68}Ga -DOTA-RM2 and clinical data.

Imaging Modality	Stratification	Positive Lesions, No. (Average)
68Ga-PSMA PET/MRI	PSA	
	<0.5	12 (0.8)
	0.5–2	14 (1.56)
	≥ 2	69 (6.27)
	PSA DT	
	<6	15 (1.67)
	≥ 6	17 (1.06)
	Not available	63 (6.3)
	GS	
	$\leq 3 + 4$	6 (1)
68Ga-DOTA-RM2 PET/MRI	$\geq 4 + 3$	84 (3.5)
	Not available	5 (1)
	PSA	
	<0.5	4 (0.33)
	0.5–2	7 (0.88)
	≥ 2	30 (2.73)
	PSA DT	
	<6	4 (0.44)
	≥ 6	4 (0.31)
	Not available	33 (3.66)
	GS	
	$\leq 3 + 4$	3 (0.6)
	$\geq 4 + 3$	36 (1.71)
	Not available	2 (0.4)

PSA: Prostate Specific Antigen (ng/mL); PSA DT: PSA Doubling Time (months); GS: Gleason Score.

A statistically significant difference in the number of lesions detected by ^{68}Ga -PSMA PET/MRI was observed when comparing patients with PSA levels below 0.5 ng/mL to those with PSA levels equal to or greater than 2 ng/mL (Mann-Whitney $U = 21.5$, $p = 0.001$) (**Figure 7a**). This difference remained significant after adjustment for multiple comparisons (adjusted $p = 0.006$). Furthermore, patients with a PSA doubling time of less than six

months exhibited a significantly higher number of detected lesions compared to those with a PSA doubling time of six months or more (Mann-Whitney U = 119, adjusted p = 0.044) (**Figure 7c**).

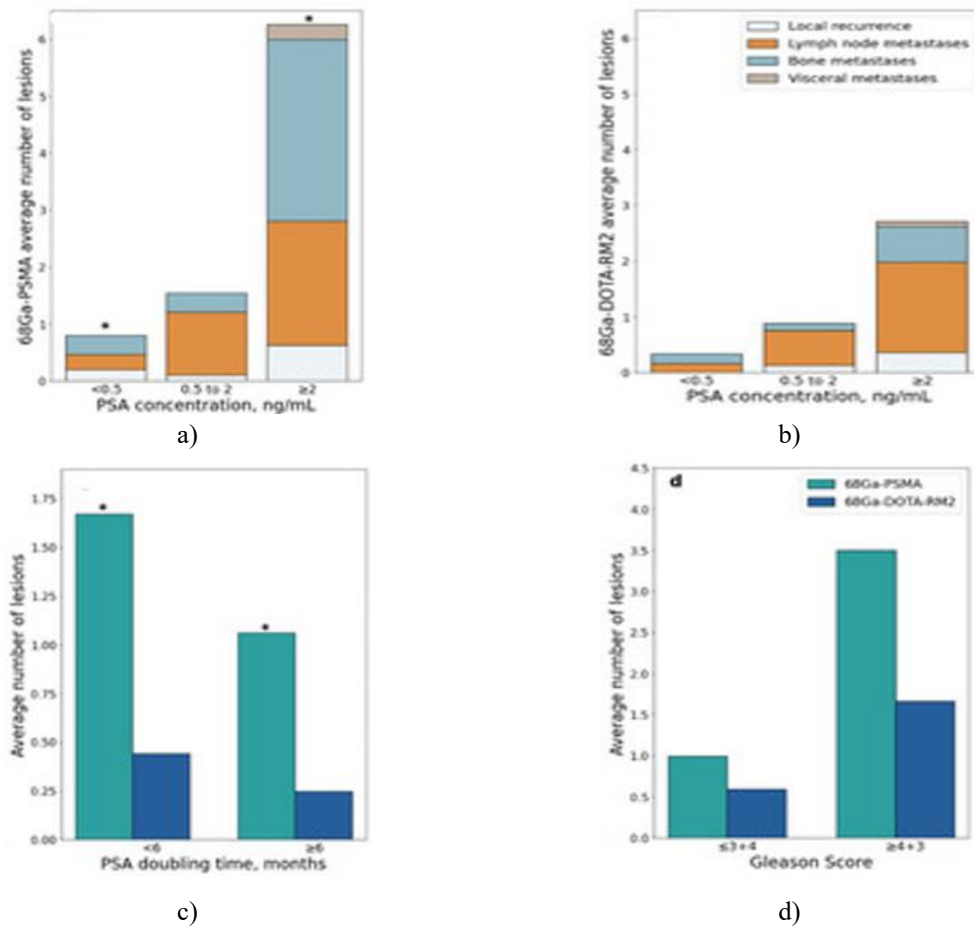


Figure 7. PET/MRI Detection Rates Stratified by Clinical Parameters

Figure 7 illustrates the detection performance of ^{68}Ga -PSMA and ^{68}Ga -DOTA-RM2 PET/MRI in recurrent prostate cancer, stratified according to clinical characteristics. Panel (a) shows the mean number of ^{68}Ga -PSMA positive lesions by anatomical site and PSA level at the time of scanning, while panel (b) presents the corresponding results for ^{68}Ga -DOTA-RM2 PET/MRI. Panel (c) depicts the average number of positive lesions for both tracers according to PSA doubling time, and panel (d) shows lesion counts stratified by Gleason score prior to radical treatment. Statistically significant differences are indicated by an asterisk (*), corresponding to p < 0.05.

Although higher PSA levels were associated with more ^{68}Ga -DOTA-RM2 positive lesions, this relationship lost statistical significance after correction for multiple comparisons (Mann-Whitney U = 46, adjusted p = 0.17; (**Figure 7b**)). Similarly, no significant differences in lesion counts were observed across Gleason score groups for either tracer (^{68}Ga -PSMA: Mann-Whitney U = 56, adjusted p = 0.43; ^{68}Ga -DOTA-RM2: Mann-Whitney U = 66.5, adjusted p = 0.65) (**Figure 7d**).

Discussion

In this study, we evaluated the diagnostic performance of ^{68}Ga -PSMA and ^{68}Ga -DOTA-RM2 PET/MRI for detecting recurrent prostate cancer after primary therapy, and investigated correlations between PET positivity and clinical as well as histopathological variables. To date, few studies have examined the combined use of these two tracers for staging and restaging in prostate cancer, often using PET/MRI and PET/CT interchangeably.

Baratto *et al.* recently conducted the largest study on dual-tracer PET in recurrent prostate cancer; however, our study offers several methodological advantages despite a smaller sample size. All participants underwent both ^{68}Ga -PSMA and ^{68}Ga -DOTA-RM2 PET/MRI scans, rather than alternating between ^{68}Ga -PSMA and ^{18}F -PSMA

as in previous studies. Patient recruitment and data collection were prospectively performed, and all findings were validated using clinical and/or instrumental follow-up.

In our cohort, ^{68}Ga -PSMA PET/MRI detected recurrent lesions in 74% of patients, whereas ^{68}Ga -DOTA-RM2 PET/MRI was positive in only 48%. Notably, nine out of ten patients who were positive on ^{68}Ga -PSMA but negative on ^{68}Ga -DOTA-RM2 were confirmed as true positives upon follow-up, contrasting with prior reports that observed similar detection rates between the two tracers. Lesion-based analysis was consistent with Baratto *et al.*, with ^{68}Ga -PSMA identifying substantially more lesions than ^{68}Ga -DOTA-RM2 (66 additional lesions in 17 patients in our study).

Detecting biochemical recurrence at low PSA levels is critical for enabling early, personalized interventions and curative local therapies. While previous studies have stratified patients into five PSA subgroups (<0.5 , $0.5\text{--}1$, $1\text{--}2$, $2\text{--}5$, >5 ng/mL), our analysis used three groups (<0.5 , $0.5\text{--}2$, >2 ng/mL) to maintain adequate sample size for statistical analysis. The absence of a significant correlation between ^{68}Ga -PSMA positivity and PSA level likely reflects the limited cohort size combined with the high sensitivity of ^{68}Ga -PSMA for low PSA values (66.7% detection for PSA <0.5 ng/mL), aligning with previous larger studies. Nevertheless, patients with PSA ≥ 2 ng/mL exhibited a significantly higher number of ^{68}Ga -PSMA positive lesions compared to those with PSA <0.5 ng/mL. Although ^{68}Ga -DOTA-RM2 PET/MRI positivity showed a trend toward higher lesion detection at increased PSA levels, the association was not statistically significant, a finding supported by ROC analysis and warranting further investigation in future studies. Consistent with prior reports, patients with slower PSA kinetics (PSA DT ≥ 6 months) were less likely to have positive ^{68}Ga -PSMA PET findings, and exhibited fewer lesions, while the same trend was not observed for ^{68}Ga -DOTA-RM2. ROC analysis indicated a moderate predictive value of PSA DT for ^{68}Ga -PSMA positivity.

The relationship between Gleason score and ^{68}Ga -PSMA PET positivity remains unclear in the literature. In our study, no significant associations were observed between PET positivity for either tracer and Gleason score.

Limitations of this study include the relatively small sample size and the absence of post-hoc histopathological correlation for all lesions, particularly those located in sites such as bone or treated directly without biopsy. Nonetheless, all PET findings were validated through clinical and instrumental follow-up. All scans were performed on a single 3 Tesla Signa PET/MRI scanner with a standardized protocol, ensuring methodological consistency. Although MR data were not analyzed for this study, future work incorporating multiparametric MRI may further enhance lesion characterization and diagnostic performance.

A potential limitation of this study is that the two PET scans were interpreted separately, and the Nuclear Medicine physicians were aware of patients' clinical histories, which could have introduced interpretative bias.

Conclusion

The use of a dual-tracer PET/MRI approach allows for more comprehensive mapping of recurrent prostate cancer following radical treatment, potentially enhancing disease characterization and informing patient management and follow-up strategies. In our cohort, ^{68}Ga -PSMA PET/MRI demonstrated a higher detection rate compared to ^{68}Ga -DOTA-RM2 for recurrent disease. Moreover, the number of lesions identified on ^{68}Ga -PSMA PET/MRI was positively associated with higher PSA levels and shorter PSA doubling times, suggesting potential prognostic relevance. In contrast, Gleason score did not show a significant relationship with PET positivity.

Acknowledgments: None

Conflict of Interest: None

Financial Support: This research was funded by the Italian Ministry of Health (Project GR-2016-02363991-EUDRACT number: 2018-001036-21). Fully hybrid 3 Tesla PET/MRI system (SIGNA PET/MRI; General Electric Healthcare, Waukesha, WI, USA) was purchased with funding from Italian Ministry of Health.

Ethics Statement: This study was approved by the Institutional Ethics Committee of IRCCS San Raffaele Scientific Institute (EudraCT 2018-001036-21) and all patients gave written informed consent to participate to the study.

References

1. Cornford P, van den Bergh RCN, Briers E, Van den Broeck T, Cumberbatch MG, De Santis M, et al. EAU-EANM-ESTRO-ESUR-SIOG guidelines on prostate cancer. Part II-2020 update: Treatment of relapsing and metastatic prostate cancer. *Eur Urol.* 2021;79(2):263–82.
2. Ploussard G, Almeras C, Briganti A, Giannarini G, Hennequin C, Ost P, et al. Management of node-only recurrence after primary local treatment for prostate cancer: Systematic review. *J Urol.* 2015;194(4):983–8.
3. Strauss DS, Sachpekidis C, Kopka K, Pan L, Haberkorn U, Dimitrakopoulou-Strauss A. Pharmacokinetics of [⁶⁸Ga]Ga-PSMA-11 in biochemical recurrence of prostate cancer. *Eur J Nucl Med Mol Imaging.* 2021;48(12):4472–82.
4. Maurer T, Eiber M, Schwaiger M, Gschwend JE. Use of PSMA-PET in prostate cancer management. *Nat Rev Urol.* 2016;13(4):226–35.
5. Han S, Woo S, Kim YJ, Suh CH. Impact of ⁶⁸Ga-PSMA PET in prostate cancer management. *Eur Urol.* 2018;74(2):179–90.
6. Fendler WP, Ferdinandus J, Czernin J, Eiber M, Flavell RR, Behr SC, et al. Impact of ⁶⁸Ga-PSMA-11 PET in recurrent prostate cancer. *J Nucl Med.* 2020;61(12):1793–9.
7. Mansi R, Fleischmann A, Macke HR, Reubi JC. Targeting GRPR in urological cancers. *Nat Rev Urol.* 2013;10(4):235–44.
8. Wieser G, Popp I, Rischke HC, Drendel V, Grosu AL, Bartholoma M, et al. Diagnosis of recurrent prostate cancer using ⁶⁸Ga-RM2 PET/CT. *Eur J Nucl Med Mol Imaging.* 2017;44(9):1463–72.
9. Baratto L, Song H, Duan H, Hatami N, Bagshaw H, Buyyounouski M, et al. PSMA- and GRPR-PET in recurrent prostate cancer. *J Nucl Med.* 2021;62(11):1545–9.
10. Jagaru A. Will GRPR compete with PSMA in prostate cancer? *J Nucl Med.* 2017;58(12):1883–4.
11. Mapelli P, Ghezzi S, Samanes Gajate AM, Preza E, Brembilla G, Cucchiara V, et al. ⁶⁸Ga-PSMA and ⁶⁸Ga-RM2 PET/MRI in high-risk prostate cancer. *Diagnostics.* 2021;11(11):2068.
12. Fassbender TF, Schiller F, Zamboglou C, Drendel V, Kiefer S, Jilg CA, et al. Voxel-based comparison of RM2-PET/CT and PSMA-PET/CT. *EJNMMI Res.* 2020;10(1):62.
13. Minamimoto R, Hancock S, Schneider B, Chin FT, Jamali M, Loening A, et al. Comparison of RM2 PET vs PSMA PET. *J Nucl Med.* 2016;57(4):557–62.
14. Panebianco V, Barchetti F, Sciarra A, Musio D, Forte V, Gentile V, et al. Prostate cancer recurrence: Role of 3-T diffusion MRI. *Eur Radiol.* 2013;23(6):1745–52.
15. Park JJ, Kim CK, Park SY, Park BK, Lee HM, Cho SW. Predicting biochemical recurrence using 3-T MRI. *AJR Am J Roentgenol.* 2014;202(3):W459–65.
16. Roach M 3rd, Hanks G, Thames H Jr, Schellhammer P, Shipley WU, Sokol GH, et al. Defining biochemical failure after radiotherapy. *Int J Radiat Oncol Biol Phys.* 2006;65(4):965–74.
17. Baratto L, Duan H, Laudicella R, Torihara A, Hatami N, Ferri V, et al. Physiological ⁶⁸Ga-RM2 uptake atlas. *Eur J Nucl Med Mol Imaging.* 2020;47(1):115–22.
18. Demirci E, Sahin OE, Ocak M, Akovali B, Nematyazar J, Kabasakal L. Normal variants of ⁶⁸Ga-PSMA-11 PET/CT. *Nucl Med Commun.* 2016;37(11):1169–79.
19. Draulans C, De Roover R, van der Heide UA, Kerkmeijer L, Smeenk RJ, Pos F, et al. Optimal window levelling for PSMA PET in prostate cancer. *Eur J Nucl Med Mol Imaging.* 2021;48(4):1211–8.
20. R Core Team. R: A language and environment for statistical computing. Vienna: R Foundation; 2019.